A FINITE ELEMENT MODELING STUDY OF THE TURKISH STRAITS SYSTEM

Özgür GÜRSES [1,2], Ali AYDOĞDU [3], Nadia PINARDI [4] and Emin ÖZSOY [1,5]

[1] Institute of Marine Sciences, Middle East Technical University, Mersin, Turkey
[2] Alfred Wegener Institute, Bremerhaven, Germany
[3] Centro Euro-Mediterraneo sui Cambiamenti Climatici, Bologna, Italy
[4] University of Bologna, Corso di Scienze Ambientali, Ravenna, Italy
[5] Eurasia Institute of Earth Sciences, Istanbul Technical University, Istanbul, Turkey

1. Introduction

The Turkish Strait System (TSS) connects the Black Sea with the Aegean Sea through the Bosphorus and Dardanelles Straits and the Sea of Marmara (Figure 1). The outflow of dense water of Mediterranean characteristics from the Bosphorus influences the long-term evolution of the Black Sea and outflow of low salinity waters from the Dardanelles Strait alters the North Aegean Sea. The TSS circulation is characterized by a two-layer exchange flow system associated with a sharp two-layer stratification. The annual freshwater flux into the Black Sea by rivers and rainfall is greater than the loss by evaporation and thus accounts for a positive freshwater balance. Ünlüata *et al.* (1990) estimated net freshwater flux (P+R-E) of 300 $km^3\ yr^{-1}$ exiting the Black Sea through the Bosphorus. The water surplus of the Black Sea drives a net barotropic flow through the TSS, superposed on top of a baroclinic exchange flow governed by hydrostatic pressure (density) differences between the two seas.

An extensive review of literature related to the currents and circulation developing in the TSS, fluxes through the Bosphorus and Dardanelles Straits and past efforts to model the TSS are presented by Gürses (2016). The modeling of the TSS has been prohibited by the requirements of fine horizontal grid size to represent straits, the need to adequately represent the complex domain geometry and the lack of available data sets. These rather stringent requirements have only permitted the system to be partially investigated. The applications have been restricted by their very nature, depending on imposed boundary conditions at their limits which are not independent of the adjoining active regions (Sözer and Özsoy, 2016). Therefore, the results are far from being fully representative of the dynamics of the entire TSS. Quasi-regular meshes have been used in the majority of earlier studies, despite the fact that mesh regularity dictates refinement in the entire domain.

The method used in the present study, presented by Gürses (2016), is to employ an unstructured mesh Finite Element Sea Ice-Ocean Model (FESOM) which already has been successfully applied to other similar cases, including the flow through the narrow straits of the Canadian Arctic Archipelago (Wekerle *et al.* 2013). The choice of the finite element discretization permits us to employ local refinement where necessary, so as to explicitly resolve the TSS at required details to address its complex dynamics in an integrated way. We extend originally closed boundaries at the external regions in adjacent seas far enough from the TSS interior to accept reservoir conditions to represent adjacent basins. In particular, we aim to answer the following questions: How significant are the improvements obtained by the model when the original relatively isolated configuration is additionally forced by surface atmospheric fluxes? How successful is the model in predicting volume transport through the Bosphorus and its variability, under the present approximations and in comparison with previous modeling efforts or measurements?

2. Study domain and bathymetry

The geometric properties of the Marmara Sea, the Bosphorus and the Dardanelles Straits with their prominent geometric features are presented in detail by various studies (Ünlüata *et al.* 1990; Gregg and Özsoy, 2002, Beşiktepe *et al.* 1994). Taking these studies into account, the model bottom topography is produced by carefully matching and combining bathymetric data from different sources, as standard datasets proved to be unsuitable for our area of interest. Gürses (2016) gives detailed information about the data sources and how they have been merged, filtered and interpolated onto the high resolution model grid.

3. Model Setup

FESOM is developed at the Alfred Wegener Institute (Danilov *et al.* 2004; Wang *et al.* 2014). It is a general ocean circulation model which solves the standard set of hydrostatic primitive equations in the Boussinesq approximation using the finite element method on an unstructured triangular surface mesh with tetrahedral volume elements. Piecewise linear basis functions are employed for velocity and tracers (in three dimensions) and sea surface elevation (in two dimensions), the so called P1-P1 scheme.

Vertical mixing is parameterized with the scheme of Pacanowski and Philander (1981) (PP), with a background vertical diffusion of 10^{-5} m^2/s for momentum and 10^{-6} m^2/s for tracers and the maximum value set to 0.005 m^2/s for either of them. Although this simple scheme suits the need of the TSS, we conducted a test simulation with the K-Profile Parameterization (KPP, Large *et al.* 1994). It is found that the results are very similar compared with the PP simulation considering the mean circulation and the stratification in the Marmara Sea. Horizontal eddy viscosity is parameterized by a biharmonic operator with a coefficient of 2.7 $x10^{13}$ m^4/s scaled with the element size cubed while horizontal eddy diffusivity is parameterized by a Laplacian operator with a coefficient of 2000 m^2/s scaled with the element (Griffies and Hallberg 2000). These values are selected based on the convergence study for second order finite difference Laplacian diffusion by Wallcraft *et al.* (2005) and set for the reference resolution of 1 degree in the model. A biharmonic operator is preferred since it involves scale selective filtering, suppressing finer scales. Laplacian is the only available scheme in FESOM for the eddy diffusion. Typical value for harmonic diffusivity of the Bosphorus, Dardanelles and Marmara Sea are calculated to be on the order of 40, 150 and 600 cm^2/s, respectively.

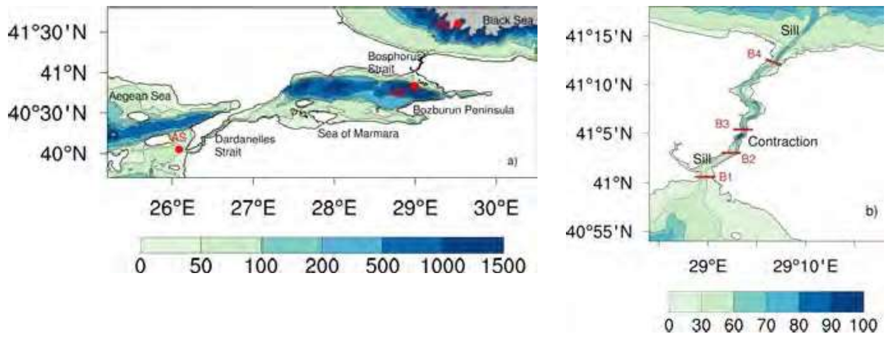

Figure 1. Location and bathymetry (in m) of a) the Turkish Strait System, b) the Bosphorus.

The model domain extends from 22.5°E to 33°E in zonal direction and 38.7°N to 43°N in meridional direction. The minimum horizontal mesh resolution in the Bosphorus and Dardanelles Straits is ~65 m and ~150 m, respectively and the maximum resolution in the Marmara Sea is set to ~1.6 km. In the adjacent regions of the Aegean and Black Seas, a resolution of ~5 km is used except for the exit and shelf areas which are better resolved. The model uses 110 z levels. The strong stratification and steep continental shelf in our implementation demands high vertical resolution in order to resolve the nonlinear hydraulic transitions, the stratified turbulent exchange flows between the upper and lower layers in the straits as well as to prevent excessive pycnocline erosion in the Marmara Sea. The minimum vertical grid spacing is set to 1 m within the first 50 m. The maximum layer thickness is not greater than 65 m in the deeper part. The time step has to be adjusted according to the minimum horizontal mesh resolution and is set to 10 s during the initialization and increased 30 s as total integration time increases.

As a first step, a lock-exchange experiment was performed (simulation BASIC), initialized with temperature and salinity data collected during the SESAME Project[1] in October 2008 (Table 1). A deep CTD cast is selected from each basin and the vertical profiles of temperature and salinity are assigned uniformly to the respective domain, are separated by a sharp discontinuity close to the mid-strait position, thereby producing a so called a lock-exchange configuration. The locations of the selected CTD stations are

[1] *Southern European Seas: Assessing and Modeling Ecosystem changes*

indicated by red dots in Figure 1. For the BASIC simulation, surface atmospheric forcing is not taken into account, setting momentum, water and heat fluxes to zero. The model is initialized from a state of rest and integrated for three months in order to assess its general behavior. No-slip boundary conditions are applied and normal velocities are to zero at all solid boundaries including those replacing the normally open boundaries the extremities of the model domain in the adjacent Black and Aegean Seas. The adjusted state of the BASIC experiment at the end of three months is used to set the initial conditions in the further simulations. In order to further evaluate model performance a one-year long hindcast simulation was performed for the year 2008 (Experiment BBExc).

Table 1. Summary of the CTD Stations selected for the lock-exchange experiment

Station ID	Latitude	Longitude	Maximum sampling depth (m)	Total station depth (m)
AS	40°02.996‘N	26°04.831‘E	67	72
MS	40°46.919‘N	28°59.971‘E	1191	1219
BS	41°36.033‘N	29°31.519‘E	1203	1271

BBExc is forced by realistic atmospheric data, but ignores net water mass fluxes from the Black Sea. The atmospheric data which drives the system are obtained from ECMWF at 6 hourly temporal and 0.125° spatial resolution for the year 2008. Bulk formulae which formerly extensively tested and utilized by the Mediterranean Forecasting System are implemented following Pettenuzzo *et al.* (2010). More details can be found in Gürses (2016). Atmospheric forcing fields are corrected against contamination by land points if they are accessed during the spatial interpolation onto the sea nodal points. The 'creeping algorithm' (also called 'sea over land') procedure is used to circumvent this problem (Kara *et al.* 2007).

4. Results

4.1. The idealized lock-exchange experiment

4.1.1. Temporal evolution of the flow in the straits

In the BASIC simulation case started from lock-exchange initial conditions, the basic gravity-driven flow through the TSS is studied without the influence of the net barotropic flow or the influence of atmospheric forcing. Time series of daily averaged kinetic energy in the Marmara Sea and volume transports respectively passing through the southern sections of the Bosphorus and Dardanelles Straits (not shown here) are shows that the net volume transport initially responds very rapidly in both shooting up in a few days and finally reaching a stable in two weeks, indicating a fast adjustment period. A slower settling time of about 30 days is observed for kinetic energy in the Marmara Sea, due to the adjustment of the larger basin.

When the model starts the barriers between the water masses located at the mid-strait positions are literally released in lock-exchange style, the density difference across the front creates a horizontal pressure gradient between basins, which is initially peaked up at the front and later spreads out as the exchange flow is initiated. Initially stagnant heavier waters start moving in the direction of the low density basin near the bottom of the Strait, while the lighter waters at the surface move in the opposite direction in compensation, as required by mass conservation. The following adjustment process establishes the sharply stratified two-layer exchange flow regime throughout the system. In the Bosphorus the along-strait bottom layer flow evolves and passes over the northern sill within the first day of integration before the Black Sea waters enter the contraction zone (Figure 2, left panel). The velocity and density fields adjust themselves to the topography. After 15 days of integration, the upper and lower layer flows are fully established in a quasi-steady state in the Bosphorus. This period is even quicker in the much wider Dardanelles Strait as a result of the lower initial density gradient between the Aegean and the Marmara Sea (Figure 2, right panel).

In close correspondence to the hydraulically controlled regime of straits, the model results clearly show the roles of strait geometry primarily determining the exchange flows through the entire TSS, by adjusting to the initial perturbation in a very short time as compared to the response of the system as a whole. The flow in the Straits adjusts indeed within less than a day or two, as a result of the suggested main hydraulic controls at the contraction and sill of the Bosphorus (roughly at 24 and 48 km, Figure 2, left panel) and the narrows at Nara Passage of the Dardanelles Strait (at about 30 km, Figure 2, right panel). Once these hydraulic controls are established, the system evolves further by density adjustments in the larger domain including the basin of the Marmara Sea. Results obtained by Sannino *et al.* (2016) from a modelling exercise using different methodology confirms the same behavior, with the hydraulic controls at the Bosphorus and Dardanelles primarily establishing the stable response of the TSS, and therefore also setting up the basic circulation regime in the Marmara Sea.

4.1.2. Marmara Sea circulation

The simulated surface circulation of the Marmara Sea averaged over the third month of integration shows a well-defined strong jet leaving the Bosphorus with core velocities of ~1.0 ms^{-1} (not shown here). This jet sets the main flow in motion and continues to the southern coast, moving parallel to the Bozburun peninsula, turning towards the northwest over the shelf region, and meandering before funneling into the Dardanelles Strait. As a result, a basin scale anticyclonic gyre is established with an average speed of 0.2 ms^{-1} and a series of small eddies (~20 km in diameter) scattered around the pathway of the main flow and at coastal embayments, with different signs of vorticity. They are separated from the main flow due to natural obstacles like islands, coastlines or rapid changes in depth. Some of the resolved eddies are identified and reported in earlier studies. These include for example the ones reported in the vicinity of the Bosphorus-Marmara Junction (BMJ, Ünlüata *et al.* 1990), a cyclonic eddy located in the southeast coast (Chiggiato *et al.* 2012) and a coastal cyclonic eddy in the north (Demyshev and Dovgaya, 2007). Besides, they are consistent with earlier observations (Beşiktepe *et al.* 1994; Gerin *et al.* 2013) and concurrent findings of Sannino *et al.* (2016). The BASIC simulation reveals that surface eddy activities are concentrated around the BMJ, namely the region of inflow into the Marmara Sea.

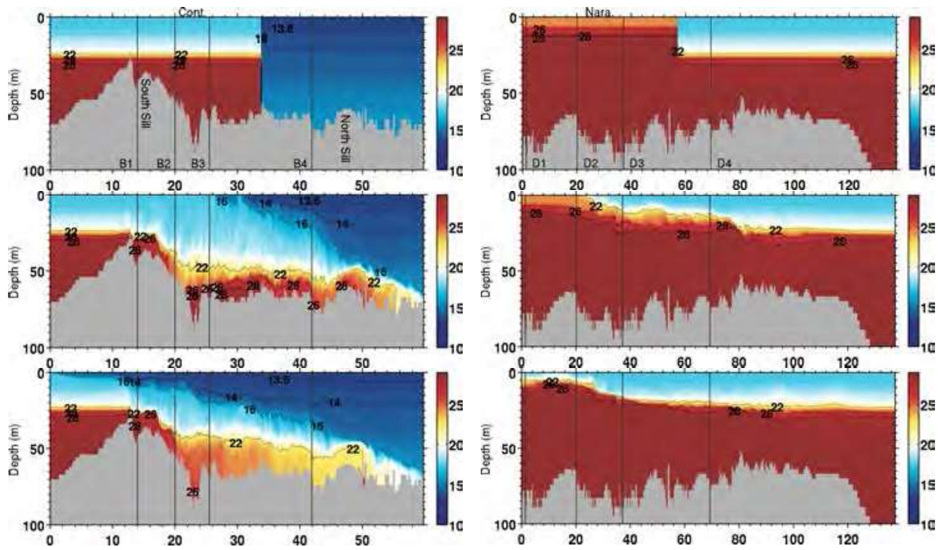

Figure 2: Snapshots of potential density along the Thalweg of the Bosphorus (from south to north, left panel) and Dardanelles (from south to north, right panel) at the initial state and after 1 and 7 days (from top to bottom). The x-axis denotes the distance in km.

The current plot at 20 m depth shows that the interfacial waters are transported with the Aegean inflow following the main channel, entering into the Marmara Sea (not shown here). In the entrance region, the flow meanders and forms two quasi-persistent eddies with a reversing sense of rotation (~15 km in diameter). At 50 m depth, the circulation pattern changes notably. The Dardanelles effluent entering the Marmara Sea follows the deep channel on the southern side of the widening section and continues straight until it hits the Marmara Island. The current at this stage bifurcates, leaving the northward branch to recirculate back into the Dardanelles along the northern half of the widening section of the Dardanelles Strait while the weaker southern branch flows around the Marmara Island before sinking deeper in the westernmost depression. There is a series of eddies moving slowly with different signs of vorticity extending down to 100 m depth (not shown here).

The simulated mid-basin pycnocline is located at 20 m on the average and does not oscillate much due to the lack of atmospheric or barotropic forcing in the BASIC experiment. Nevertheless, the 10 m circulation map shows that the flow enters the Bosphorus at this level. This indicates that the pycnocline is tilted upwards towards the Bosphorus and the jet leaving it is confined to the upper 10 m.

4.2. Simulations with realistic atmospheric forcing

The main driving forces in the Turkish Strait System are the atmospheric forcing and the Black Sea freshwater input (Gregg and Özsoy, 2002). The response of the Marmara Sea to both of these factors has been previously taken up by Chiggiato *et al.* (2012) and Demyshev and Dovgaya (2007), although the influence of strait dynamics has been completely ignored and only represented as inflow / outflow in their work. In recognition of the importance of these external factors we take solely the atmospheric forcing into consideration in this section and leaving the Black Sea freshwater forcing aside for further studies. Our model open boundaries are closed in the Aegean and the Black Seas, we take into account the effects of neighboring basins by attempting to include the atmospheric forcing as described earlier.

The surface circulation and salinity fields simulated by BBExc averaged for the months of April and October 2008 are shown in Figure 3. The circulation in April is characterized by eastward flow in the northern part of the Marmara Sea, and a westward flow in the southern part of the basin, and very little eddy activity. In contrast, observations show a strong anticyclonic gyre dominating the eastern part of the Marmara Sea driven by the Bosphorus jet. The difference in the circulation pattern in April between the simulation and the observations is due to missing Black Sea freshwater forcing. This clearly demonstrates that substantial changes in the surface circulation of the Marmara Sea by energizing the Bosphorus jet is expected to be driven by the freshwater excess of the Black Sea. In other words, the Bosphorus throughflow is indicated to be a significant driver of the seasonal circulation of the Marmara Sea. In October, BBExc simulation shows strong westward surface flow associated with cyclonic eastern and anticyclonic western eddies. As a result, the main flow diverted on to the southern shelf and passes through the island groups located in the vicinity of the Dardanelles entrance.

Regarding surface salinity fields, the BBExc simulation shows differences in the studied months of April and October 2008. Waters exiting the Bosphorus fills almost the entire eastern Marmara basin under the calm wind conditions in April. In October, fresher Bosphorus originated waters are mostly trapped in the vicinity of the northern coast. This shows that the circulation reacts faster to the changes in atmospheric conditions transmitted by the Bosphorus jet, whereas the adjustment of the salinity field depends on a multiplicity of other factors on the longer term.

The adjustment in the average position of the simulated $\sigma_t = 25$ surface in the Marmara Sea (not shown here) reveals the role of winds on interface depth. The correlation between the BBExc simulation and the measurements reveals that atmospheric forcing is responsible for high frequency variability in both simulations. In particular, the storm activities are responsible for the changes of up to 2 m in the interface depth within a few days. The absence of barotropic forcing results in a shallower interface position compared with the observations. Additionally, a weaker seasonality of the pycnocline is observed showing that the position of the interface is probably controlled by the freshwater balance in the Black Sea.

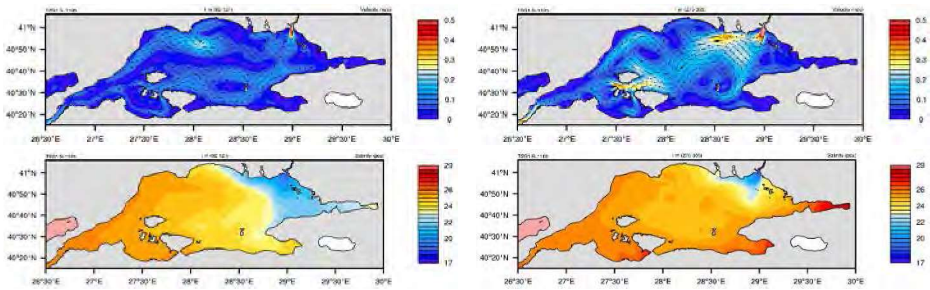

Figure 3. Simulated surface circulation in ms-1 (upper panel) and salinity in psu (lower panel) in the Marmara Sea averaged over April 2008 (left) and October 2008 (right) for experiment BBExc.

The observations were obtained during the SESAME Marmara Sea cruise separated into two legs of 4 days duration each. The first leg was carried out from 11 to 14 April 2008, and the second leg from 1 to 4 October 2008. T-S diagrams of water masses in the Marmara Sea are presented in Figure 4. The observed salinity and temperature profiles averaged over all CTD stations in the Marmara Sea are compared with the model results obtained from the BBExc simulations. The comparison is carried out for the upper 50 m of the water column, where most seasonal changes occur. Comparison of water properties below this depth requires longer simulations since the associated time scales are longer, based upon mean residence time estimates of 6-7 years, Ünlüata *et al.* (1990). The observations (dashed lines) show that the halocline and thermocline are positioned deeper in spring than autumn, evidently due to the increased freshwater input into the Black Sea in spring. The thermocline and halocline estimated from both simulations are in agreement with their observed structure in the Marmara Sea.

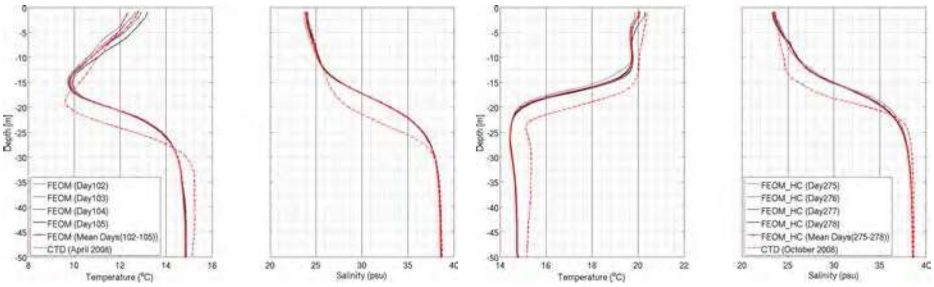

Figure 4. Vertical profiles of temperature and salinity in the surface layers of the Marmara Sea averaged over all stations. Model results are interpolated onto the position of the CTD stations for simulation BBExc. Red dashed lines represent the observations. Black and red solid lines indicate daily and cruise time averaged simulations, respectively. Left panel: April 2008, Right panel: October 2008.

Figure 4 compares the observed and the average simulated temperature and salinity fields in vertical water column. The simulated profiles during the measurement period are also depicted. The surface temperature discrepancy between simulation and observation does not exceed 0.5°C. The temperature minimum ~ 4 m above the thermocline in April 2008 is captured in the simulation. Below the thermocline, on the average across the Marmara Sea, the model predicts slightly colder water (by ~15°C) compared to the observations, due to the influences propagated from the horizontally uniform initial temperature profile imposed in the small external domain in the Aegean Sea. The salinity in the surface and deeper layers are simulate well comparing to the measurements. Lack of barotropic forcing due to Black Sea inflow possibly reveal such kind of uniform surface salinity which in reality may not be too uniform and because the Black Sea not physically well represented in the present model. This reveals that the model is capable of ensuring high skill in representing the gradients of temperature and salinity fields in vertical. However, there is a bias in the positioning of the aforementioned fields. This is linked to the missing freshwater forcing from the Black Sea which leads the rise of the interface in the Marmara Sea.

The model performance is further assessed by means of root-mean-square error (RMSE) comparison of properties between the model and the observations, computing errors over each CTD profile in the depth range 0 - 50 m (Figure 4). Despite the initialization with simple profiles, BBExc results are in agreement with the observation for both measurement periods (Figure 5). The source of the error is the misplacement of the halocline and thermocline which are too close to the surface. The error field is independent from the representation of hydrological properties of the Black Sea water influencing surface layers of the Marmara Sea. Temperature errors for both hindcast experiments do not differ much for each measurement periods.

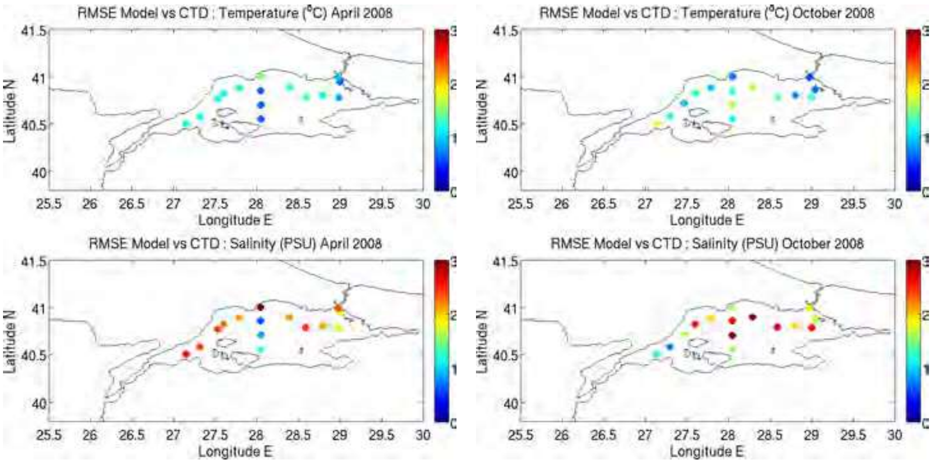

Figure 5. Accumulated root-mean-square errors between simulated and observed temperature (upper panel) and salinity profiles (lower panel) in the Marmara Sea for April 2008 (left) and October 2008 (right).

4.2.1. Model assessment with focus on the Bosphorus Strait

In the following we concentrate on the more realistic simulation, BBInc, and further investigate the ability of the model to simulate flow features and transports in the Bosphorus Strait. We compare time series of modeled and observed velocities in the southern Bosphorus, based on observations obtained from Jarosz *et al.* (2011). Observations indicate that the along-strait velocity component of the southern Bosphorus (at the middle of Section B1) varies considerably throughout the year 2008. In the simulation, the mean depth of the zero-velocity isotach is 8.75 m, shallower than the observed depth of 13.5 m reported by Jarosz *et al.* (2011). The maximum simulated along-strait current speed in the upper layer (1.31 ms^{-1}) is considerably lower than the observed value of 2.3 ms^{-1} (Jarosz *et al.* 2011).

Measurements of volume transports through the Bosphorus and Dardanelles straits were conducted from September 2008 to February 2009 during the experiments reported by (Jarosz *et al.* 2011). A comparison of these observations with the simulated transport time series is presented in Figure 7. The correlation coefficients between model and observations for the upper and lower layer and net daily mean volume transports through the northern Bosphorus respectively are $r_{upper}=0.75$, $r_{lower}=0.68$ and $r_{net}=0.74$. These results reveal that the model is consistent with the measurements and able to capture the variability of the transport.

During the same period, the simulated net mean transport (49.7 $km^3\ yr^{-1}$) into the Marmara Sea compares relatively well with the observed net flux (86.3 $km^3\ yr^{-1}$) reported by Jarosz *et al.* (2011). However, simulated upper layer and lower layer transports (240.1

km^3 yr^{-1} and 190.4 km^3 yr^{-1}, respectively) are much lower that the observed transports (359.9 km^3 yr^{-1} and 273.6 km^3 yr^{-1}, respectively) for the period Sep-Dec 2008. The amplitude of the fluctuating components of transport in the model results is lower compared to that in the measurements. This is due to missing Black Sea freshwater contribution, the relatively coarse resolution of the atmospheric forcing and limited model domain in the Black and Aegean Seas.

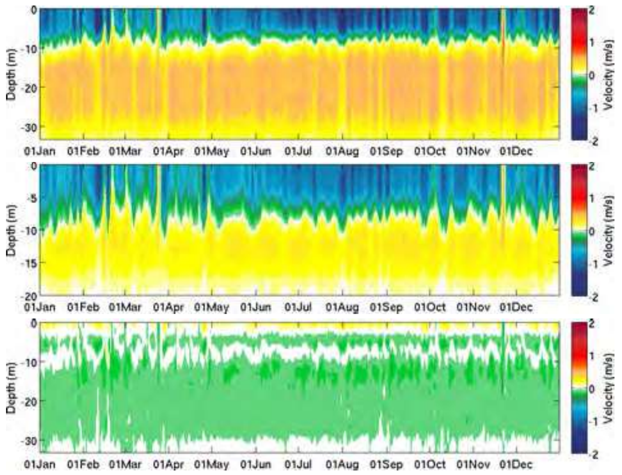

Figure 6. Time series of the simulated along-strait velocity profiles (ms^{-1}) in the middle of the Section B1 (top) and close to the Asian coast on Section B1 (middle) and cross-strait velocity profiles in the middle of the Section B1 (bottom) for the year 2008.

4.2.2. Blocking events

Under normal conditions, a progressive decrease occurs in the thickness of the upper layer starting from the northern end of the Bosphorus (45 - 50 m over the northern sill) until the Dardanelles-Aegean Sea Junction (~10m). The upper layer thickness in the Marmara Sea is typically around 25 m. Strong northerly winds combined with higher sea level difference between the Aegean and the Black Sea may deepen the interface position in the northern exit of the Bosphorus, leading to blocking of the lower layer flow which can last a few days (termed "lower layer flow reversals", LLR). Conversely, strong southerly wind in combination with a decrease in sea level difference can arrest the surface layers and even reverse it for several days (termed "upper layer flow reversals", ULR, Latif *et al.* (1991); Jarosz *et al.* (2011)).

An upper layer blocking event occurring on the dates of November 21 and 22, 2008 in the model (Figure 6). The blocking event has created a pulse of northward owing net currents through the Dardanelles and Bosphorus, evident from surface currents displayed on the left hand side panels of Figure 8. For comparison, the simulated monthly mean surface currents in November 2008 are shown in the right hand side panels of Figure 21, indicating the average situation which is only disturbed during the blocking event.

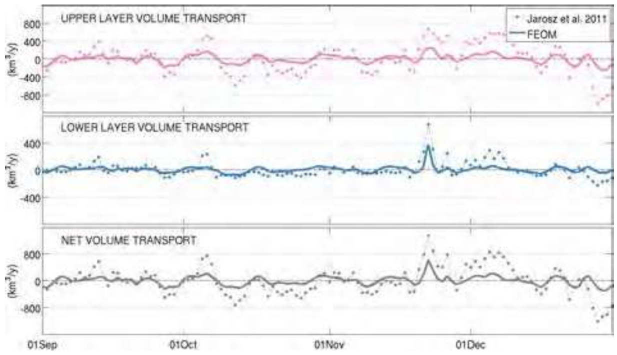

Figure 7. Time series of detrended simulated (solid line) and observed (dotted line) volume transport through section B4 (Northern Bosphorus). Observations are taken from Jarosz *et al.* (2011).

In fact, the currents on November 21, 2008 correspond to an explosive cyclone passing over the region characterized by strong southwesterly winds. The effects of this storm on the TSS and its dynamic response to the atmospheric forcing has been analyzed in some detail by Book *et al.* (2014)), based on the measurements campaign of Jarosz *et al.* (2011)). Both the observations and the model results indicate a complete change in the flow direction as the upper layer is blocked and pushed backwards. In the Bosphorus, the simulated currents exceed 1 ms^{-1} starting from the southern sill until north of the contraction. The flow reversal reaches as far as the Bosphorus-Black Sea Junction. A similar flow reversal is observed in the Dardanelles (Figure 8) with a one-day time lag after the Bosphorus. The circulation in the Dardanelles displays a channel-wide cyclonic recirculation cell near its southern exit.

During the year 2008, the ECMWF atmospheric data reveals that there were several strong storms (lasting 3 - 5 days) passing over the TSS region. Observations indicate several upper layer blocking events from September to December 2008, Jarosz *et al.* (2011)). The upper layer flow reversals observed during the periods 1 - 7 October 2008 and 20 - 22 November 2008 are clearly represented in the simulation (Figure 6). It should be noted that lower layer blocking has not been observed during the time period September to December 2008, neither in observations nor in our simulation.

5. Conclusions

We have set up and tested the multi-resolution ocean model FESOM for the limited but complex domain of the TSS, using a particularly enhanced resolution in the Bosphorus and Dardanelles Straits in order to adequately represent the energetic processes in these regions in the overall dynamics of the coupled system. Based upon an initial adjustment of the lock-exchange configuration to quasi-steady state in the BASIC experiment, BBExc simulation dwells upon the impacts of realistic atmospheric forcing (BBExc) excluding the Black Sea freshwater budget on the dynamics of the TSS.

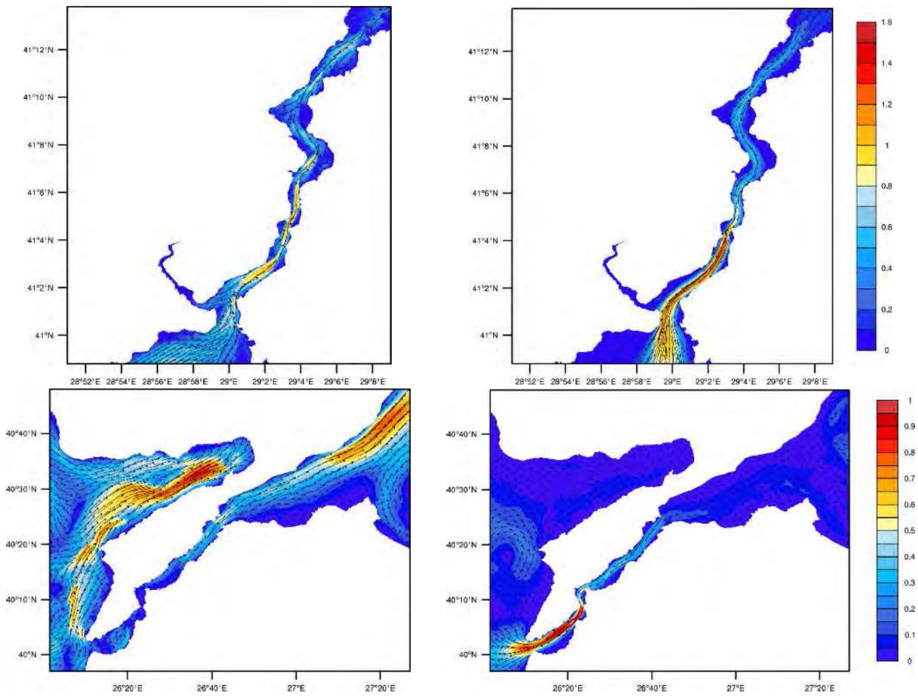

Figure 8. Simulated surface currents (in ms^{-1}) on November 21, 2008 in the Bosphorus (top left) and on November 20, 2008 in the Dardanelles (bottom left) and surface currents averaged over November 2008 (right).

Our BASIC simulation produced a general circulation and a stable stratification in the Marmara Sea consistent with previous measurements. Sensitivity experiments showed a reasonable compromise between resolution and computational cost, which the selected model configuration seemed to satisfy. The pycnocline depth in the Marmara Sea in BBExc showed a rising trend towards the surface in the absence of net volume transport through the Bosphorus. This trend is probably controlled by the Black Sea freshwater budget. Comparing the simulated surface circulation in the Marmara Sea in both experiments showed the circulation to be dominated by the Bosphorus inflow and modulated by atmospheric forcing. The results were compared with respect to observed salinity and temperature CTD profiles in the Marmara Sea and transport measurements in the Bosphorus. The comparison with transport measurements in the Bosphorus revealed very strong model skill in representing the variability despite low the upper layer and lower layer mean transport and standard deviation were lower compared to the observed values.

To conclude, the novelty in this work is the ability to uniformly represent the integral behavior of the TSS, which demonstrates the advantage of the multi-resolution approach. We proved that one key forcing functions is the atmospheric forcing and it is essential to provide realistic fluctuations of the pycnocline depth in the Marmara Sea.

The model can be improved in several ways. (1) An improved variability and a stable pycnocline depth with the correct seasonal cycle and net transport through the Bosphorus is only possible by including the freshwater budget. (2) The comparison of transports revealed the significance of the atmospheric forcing on the high frequency variability. In our simulations, we applied a correction to the sea points along the shore line to hinder the contamination of the land based points in the ECMWF wind field. Higher resolution atmospheric forcing both in spatial and temporal sense would be more justifiably needed to accurately represent forcing in this small and complex region on the passageway of atmospheric cyclones. (3) So far, the choice for the initial and boundary conditions were idealized. The model setup is now ready to perform multi-year simulations with realistic initial conditions. (4) The current model setup revealed a significant correlation between the sea level difference between Black and Aegean Seas and transport through the southern Bosphorus ($r = -0.87$), and this should be explored further. (5) More realistic surface water, heat and salinity boundary conditions and the incorporation of nonlinear free surface approach recently developed for the FESOM are all too relevant for the TSS and its inter-basin coupling, and are expected to improve results in the future. (6) Given the importance of the sea level difference on the TSS transports, the model domain should be extended to include the entire Black and Mediterranean Seas. We expect that a more realistic simulation of SSH in the two basins should improve the simulated transports.

Acknowledgements

This study was initiated as part of a PhD at the Institute of Marine Sciences, METU (IMS-METU) and continued later at the Alfred Wegener Institute (AWI) and the Istituto Nazionale di Geofisica e Vulcanologia (INGV), through support provided to the first author as research assistant at IMS - METU and Helmholtz Foundation grantee under bilateral agreement with the Turkish Scientific and Technical Research Council (TÜBİTAK), followed by an assignment at INGV. Limited travel support was provided under project 110Y344 supported by TÜBİTAK. We also acknowledge the support by the SESAME, MyOcean2 and MyOcean Follow On European projects in which the authors participated. CTD and other data used in this study have been obtained in collaboration with the research personnel of the IMS - METU and during research cruises on board the R/V BİLİM. We thank E. Jarosz for providing observed transports through the Bosphorus and Dardanelles. We would like to thank to C. Wekerle for her preview of the paper and valuable advice in writing.

References

Beşiktepe, Ş.T., Sur, H.İ., Özsoy, E., Latif, M.A., Oğuz,T. and Ü. Ünlüata 1994. The circulation and hydrography of the Marmara Sea. *Prog. Oceanogr*. 34: 285-334.

Book, J.W., Jarosz, E., Chiggiato, J. and Ş. Beşiktepe 2014. The oceanic response of the Turkish Straits System to an extreme drop in atmospheric pressure. *J. Geophys. Res. Oceans* 119: 3629-3644.

Chiggiato, J., Jarosz, E., Book, J.W., Dykes, J., Torrisi, L., Poulain, P.M., Gerin, R., Horstmann, J. and Ş. Beşiktepe 2012. Dynamics of the circulation in the Sea of Marmara: Numerical modeling experiment and observations from the Turkish strait system experiment. *Ocean Dynam.* 62: 139-159.

Danilov, S., Kivman, G. and J. Schröter 2004. A finite-element ocean model: principles and evaluation. *Ocean Model.* 6(2): 125-150.

Demyshev, S.G. and S.V. Dovgaya 2007. Numerical Experiment aimed at modeling the hydrophysical fields in the Sea of Marmara with regard for Bosphorus and Dardanelles. *Physical Oceanography* 17: 141-153.

Gerin, R., Poulain, P.M., Beşiktepe, Ş.T. and P. Zanasca 2013. On the surface circulation of the Marmara Sea as deduced from drifters. *Turkish Journal of Earth Sciences* 22(6).

Gregg, C.M. and E. Özsoy 2002. Flow, water mass changes and hydraulics in the Bosphorus. *J. Geophys. Res.* 107: 3016.

Griffies, S.M. and R.W. Hallberg 2000. Biharmonic friction with a Smagorinsky-like viscosity for use in large-scale eddy-permitting ocean models. Mon. *Weather Rev.* 128: 2935-2946.

Gürses, Ö. 2016. Dynamics of the Turkish Straits System – A Numerical Study with a Finite Element Ocean Model Based on an Unstructured Grid Approach, PhD Thesis.

Jarosz, E., Teague, W.J., Book, J.W. and Ş.T. Beşiktepe 2011. On flow variability in the Bosphorus Strait. *J. Geophys. Res.* 116: C08038.

Kara, A.B., Wallcraft, A.J. and H.E. Hulburt 2007. A correction for land contamination of atmospheric variables near land-sea boundaries. *J. Phys. Oceanogr.* 37: 803-818.

Large, W., McWilliams, J. and S. Doney 1994. Oceanic vertical mixing: A review and a model with nonlocal boundary layer parameterization. *Rev. Geophys.* 32: 363-403.

Latif, M.A., Özsoy, E., Oğuz, T. and Ü. Ünlüata 1991. Observations of the Mediterranean inflow into the Black Sea. *Deep-Sea Res.* 38: 711-723.

Pacanowski, R. and S. Philander 1981. Parameterization of vertical mixing in numerical models of tropical oceans. *J. Geophys. Res.* 11: 1443-1451.

Pettenuzzo, D., Large, W.G. and N. Pinardi 2010. On the corrections of ERA-40 surface flux products consistent with the Mediterranean heat and water budgets and the connection between basin surface total heat flux and NAO. *J. Geophys. Res.* 115: C06022.

Sannino, G., Sözer, A. and E. Özsoy 2016. A high-resolution modelling study of the Turkish Straits System. *Ocean Dynam.* (submitted).

Sözer, A. and E. Özsoy 2016. Modeling of the Bosphorus exchange flow dynamics. *Ocean Dynam.* (submitted)

Ünlüata, Ü., Oğuz, T., Latif, M.A. and E. Özsoy 1990. On the physical oceanography of the Turkish Straits. In: L.J. Pratt (Ed) Physical oceanography of the Sea Straits. NATO/ ASI Series, Kluwer Academic Publishers, Dordrecht, 43-64 pp.

Wallcraft, A.J., Kara, A.B. and H.E. Hurlburt 2005. Convergence of Laplacian diffusion versus resolution of an ocean model. *J. Geophys. Res.* 32: L07604.

Wang, Q., Danilov, S., Sidorenko, D., Timmermann, R., Wekerle, C., Wang, X., Jung, T. and J. Schröter 2014. The finite element sea ice-ocean model (FESOM) v.1.4: formulation and ocean general circulation model. *Geosci. Model Dev.* 7: 663-693.

Wekerle, C., Wang, Q., Danilov, S., Jung, T. and J. Schröter 2013. Freshwater transport through the Canadian Arctic Archipelago in a multi-resolution global model: model assessment and the driving mechanism of interannual variability. *J. Geophys. Res.* 118: 4525-4541.